Severe Accident Management Measures for a Generic German PWR. Part II: Small-break loss-of-coolant accident

Jobst, M.; Wilhelm, P.; Kozmenkov, Y.; Kliem, S.;

Originally published:

September 2018

Annals of Nuclear Energy 122(2018), 280-296

DOI: https://doi.org/10.1016/j.anucene.2018.08.017

Perma-Link to Publication Repository of HZDR:

https://www.hzdr.de/publications/Publ-26573

Severe Accident Management Measures for a Generic German PWR. Part II: Small-break loss-of-coolant accident

M.Jobst*, P.Wilhelm, Y.Kozmenkov, S.Kliem

Helmholtz-Zentrum Dresden-Rossendorf (HZDR) e.V.
Institute of Resource Ecology
Reactor Safety Division
Bautzner Landstraße 400, 01328 Dresden, Germany

E-mail addresses:
m.jobst@hzdr.de; p.wilhelm@hzdr.de; y.kozmenkov@hzdr.de; s.kliem@hzdr.de

* Corresponding author. Present address:
Helmholtz-Zentrum Dresden-Rossendorf (HZDR) e.V.
Institute of Resource Ecology
Reactor Safety Division
Bautzner Landstraße 400
01328 Dresden
Germany

Highlights (for review)

- Investigation of SBLOCA severe accident transient with ATHLET-CD code.
- Mobile pump injection to reactor coolant system under various core conditions.
- Assessment of mobile pump injection combined with primary side depressurization.
- Quantification of releases of fission products and hydrogen.
- Proposal of a preferred mobile pump injection strategy based on simulation results.

Abstract

This paper focuses on the analysis of severe accident management measures for a generic German PWR of type Konvoi. A nuclear power plant model based on the severe accident code ATHLET-CD was developed in order to assess the code applicability for simulation of accident scenarios with core degradation. It was applied for investigation of two main groups of accident scenarios: station blackout and small-break loss-of-coolant accidents.

Part II of the series of two papers is focused on the analysis of the plant response in case of a hypothetical small-break loss-of-coolant accident (SBLOCA with 50 cm² leak in cold leg of pressurizer loop). Due to failure of components of the emergency core cooling system, the accident develops into a severe accident scenario with core melt and reactor pressure vessel failure. On the basis of simulations performed with ATHLET-CD Mod 3.0 Cycle A, late coolant injection to the primary circuit with a mobile equipment (bleed and feed with low pressure pump) is assessed. Two injection points are investigated: injection to cold leg and injection to hot leg. As in SBLOCA scenarios the primary pressure might remain high that injection by low pressure systems is not effective, the influence of additional primary side depressurization (PSD) is investigated.

The simulations show, that mobile pump injection significantly reduces the amount of the released fission products and hydrogen, if it is started within 75 min after the core exit temperature (CET) exceeded 400 °C. Without PSD, fuel melt can be prevented if the mobile pump is started immediately when CET > 650 °C, but release of fission products can only be prevented if early pump injection is combined with PSD. An injection strategy with a delayed PSD (delayed till the mobile pump is available) and injection to hot leg, immediately started after PSD, provides the most effective cooling of the core until approximately 50 min after CET > 400 °C, with lowest fission product releases and longest grace time to prevent melt relocation to the lower head. This strategy also shows the lowest hydrogen releases till approx. 35 min after CET > 400 °C. Later on, up to 45 % higher hydrogen mass is released compared to cold leg injection.

Keywords: Severe accident analysis, SBLOCA, PWR, accident management measures

1. Introduction

Part II of the paper (see (Wilhelm et al., xxxx), submitted together with this paper), deals with small-break loss-of-coolant (SBLOCA) analyses for a generic German PWR Konvoi. The reactor model of a generic German PWR of type Konvoi described in part I and described in more detailed in (Tusheva et al., 2015; Jobst et al., 2017a) is used in the current paper to investigate the plant response in case of a hypothetical SBLOCA accident scenario with 50 cm² leak size. Additional failure of active components of the emergency core cooling system (which are described later) are assumed, so that the SBLOCA scenario develops into a severe accident scenario with core melt, relocation of the melt into the lower head of the reactor pressure vessel (RPV) and failure of the RPV.

A SBLOCA scenario for a 1300 MW Konvoi, which develops into a severe accident was investigated by Reinke et al. (2010) by means of two alternative severe accident codes MELCOR and ASTEC. The focus there was on the comparison between the transient evolutions predicted by both codes, which revealed differences in the predicted timings till RPV failure of approximately 25 % (1½ hours). Both codes showed also qualitatively different evolution of the transient (early release of fission products was predicted by MELCOR approximately 15 minutes into the transient vs. later beginning of release at more than 3 hours was predicted by ASTEC). The assumptions differ from the current study (e.g. in the current study secondary cool-down is assumed to be unavailable and the emergency core cooling systems are available till the depletion of the flooding pools). Therefore, the results of the base scenario presented in the current study (without applied accident management measures (AMM)) cannot be directly compared to the results from (Reinke et al., 2010).

LOCAs in a generic Konvoi, that develop into severe accidents, were also recently studied by means of ASTEC code simulations, for small leaks with 10 cm² leak size (Gomez-Garcia-Torano et al., 2017b) and for medium breaks (Gomez-Garcia-Torano et al., 2017a). In these studies, AMM such as bleed and feed to primary side and primary side depressurization (PSD) were investigated. Medium-break LOCAs in a generic Konvoi were also studied by means of ATHLET-CD code simulations (Trometer et al., 2014; Trometer et al., 2015; Trometer, 2016). The focus there was on the reflooding of a degraded core by ECCS injection and middle pressure pumps.

The focus of the current study is on the assessment of AMM, which can be applied to PWRs to prevent the development of the above mentioned SBLOCA scenario into a scenario with core melt or to mitigate the consequences of an already ongoing core-melt (stop of core melt progression, limitation of fission product releases, possible prevention of further consequences like the failure of the vessel). Therefore, the AMMs described and analyzed in part I of the paper (Wilhelm et al., xxxx) are now applied to the SBLOCA scenario to investigate their applicability and effectiveness for a wider range of possible severe accident scenarios. In particular, the late injection by a mobile (fire pump) system into the primary side of the reactor cooling system (RCS) will be investigated under several core conditions with already elevated core temperatures as well as partly molten core or under conditions, when part of the core is already relocated to the lower head of the RPV.

For our analyses we assume that from a certain point of the transient, no further active or passive emergency core cooling system (ECCS) is available (see details of our assumptions given in section 3). Instead, a typical fire pump system, similar to those available on the market, will be used to inject additional coolant to the core. Such mobile fire pump systems are usually designed for a pressure head of 16 bar according to standards like German standard for fire hoses (DIN 14811-1, 1990). As the primary pressure usually remains higher in the case of primary circuit leaks with small leak sizes, the effectiveness of injection by such a mobile pump system may be limited. Therefore, as additional AMM, primary side depressurization (PSD) is investigated, whether it can improve the effectiveness of the mobile pump injection (MPI). Several questions arise about how the injection with mobile pump system should be carried out in the most efficient way:

- What is the latest core state at which MPI has to be started that the fuel cladding will remain intact and the release of fission products to primary circuit coolant can be prevented?
- What is the latest core state at which the MPI has to be started that melting of fuel or its relocation from core to lower plenum can be avoided?
- If part of the core is already slumped down to the lower plenum followed by the formation of a molten pool, how much of the decay heat can be removed from the molten pool by the injected water and can the vessel wall be maintained intact?
- Shall the mobile pump system be connected to the cold leg or the hot leg of the reactor cooling system?
- Can the injection lead to additional pressure loads and/or enhanced oxidation with hydrogen production?
- When should PSD be applied and does it always lead to an enhanced injection to the RCS and a less severe progression of the accident?

These questions will be discussed by means of calculation results obtained using the above mentioned ATHLET-CD model of a generic PWR (Konvoi-like). ATHLET-CD Mod 3.0 Cycle A has been used for the current analyses.

2. Overview on the model and modifications needed to perform the SBLOCA analyses

Fig. 1 depicts a nodalization scheme of the primary and secondary circuit of the ATHLET-CD model, which has been created as a two loop model: a triple loop which models three loops of the four loop real Konvoi plant (named as Loop 1 in Fig. 1) and a single loop connected to the pressurizer (named as Loop 2 in Fig. 1). Within the RPV, the downcomer, lower plenum, core, upper plenum and upper head are modelled. The thermal-hydraulics of the core is represented by six parallel flow channels and a reflector channel. Each channel represents one concentric ring of the core and the flow channels are interconnected by cross connection objects. The 57900 fuel rods and 1464 control rods of a Konvoi PWR are modelled by six representative fuel rods and five representative control rods, one representative fuel rod and one control rod per core section, except for the outermost core section which only contains fuel rods. The fuel and the control rods are modelled by the ATHLET-CD ECORE module. The phenomena covered by the ECORE module are summarized in part I of the paper (Wilhelm et al., xxxx). Also for the analyses in the current paper, the decay heat is implemented as tabular values based on a preceding simulation (see section 3 in part I of the paper). A full list of the applied core degradation parameters is given in (Jobst et al., 2016). Furthermore, it has to be mentioned, that the release of fission products (FP) is simulated by the module FIPREM. It is assumed that the released FPs are transported away immediately (through the leak or the pressurizer valves in case of PSD applied as AMM) and therefore do not further contribute to the heat-up of the primary circuit.

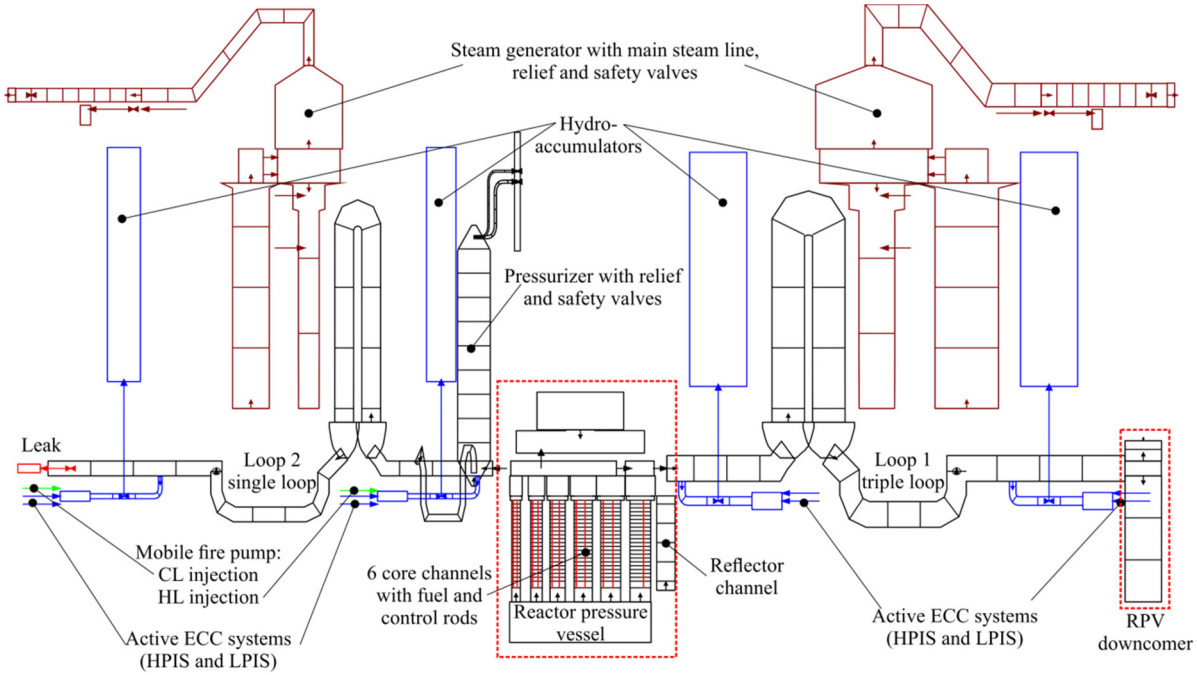

Fig. 1. Nodalization scheme of the generic Konvoi model with location of the leak and mobile pump injection points.

ATHLET-CD simulates the core material relocation inside the core region on the basis of a candling model (Trambauer et al., 2004): molten material flows from failed rods downwards to colder regions and refreezes there (formation of crust). This can lead to blockages in the core, where additional material is accumulating above. This can cause the formation a molten pool, which is surrounded by a crust. This crust may fail and the molten material may be relocated to the lower head. In ATHLET-CD the initiation of molten material relocation to the lower head has to be defined by the user and from that moment on, the processes in lower head (formation of a homogenous molten pool covered by water, damage and failure of the vessel wall) are treated by the lower head module AIDA (Bals et al., 2012; Austregesilo et al., 2013). In the current model, an early initiation criterion has been selected (start of continuous material relocation at 35 t core melt mass, approx. 20 % of the total core, shortly after occurrence of the first ceramic melt which is a necessary constraint for the application of the continues relocation model, see (Austregesilo et al., 2013)). This is conservative in the sense that the lower head is penetrated by the heat load as early as possible. A first comparison of the differences found in the course

of the transient for two different relocation criteria was presented in (Jobst et al., 2017b). There it was shown that late relocation initiated from 100 t core melt mass can lead to time shifts in the course of transient of up to 45 minutes.

As already stated in part I of the paper, the lower head module AIDA contains three different models to calculate the damage of the vessel wall (Austregesilo et al., 2013). These are the ASTOR approximation (Schaaf et al., 1999), for which the implemented data is limited to pressures above 3.0 MPa, the Larson-Miller approach and a third rupture model, which takes plastic rupture and creep rupture into account (Autrusson and Combescure, 1999; Pandazis, 2017). The investigated SBLOCA scenario is a low pressure scenario with pressures around 1.0 MPa during the late in-vessel phase, and even lower than 1.0 MPa for cases with PSD (see the results in sections 4 and 5). According to Altstadt (2012) creep processes are only significant for high temperatures and pressures above 1.0 MPa. Therefore the plastic rupture model was selected to determine the RPV failure times. For purpose of comparison, the results of the Larson-Miller approach will be also given in the paper, for which the rupture times were assessed during the post-processing of the data (on the basis of the equations implemented in ATHLET-CD (Pandazis, 2017), and pressures and temperatures taken from the ATHLET-CD results). As will be seen from the results, this approach leads to rupture times much beyond the total simulation time for most of the cases.

For LOCA scenarios as discussed in this paper, the location, orientation and geometry of the leak is of particular importance to describe the pressure reduction and loss of primary coolant in a correct manner. Based on a parameter study (Schäfer et al., 2014; Jobst et al., 2017a), a leak in the cold leg of the single loop, close to the RPV outlet, and with 50 cm^2 leak size has been selected for the current analyses. The leak is defined as a horizontal junction, branching off the main coolant pipe at its center elevation. From the available ATHLET critical flow models, the CDR1D model was used, as it is the one that can cover the complete range of thermal-hydraulic states that can occur at the leak during the investigated transients: from the discharge of sub-cooled liquid which occur at the beginning of the transient or later, when ECC systems are working till the discharge of strongly superheated vapor, which can occur later during the severe accident transient after core heat-up. The CDR1D model is used to describe the region upstream of the leak and the critical flow at the discharge orifice, which is assumed to be directly at the surface of the main coolant pipe. As the critical flow can be treated as quasi-stationary, it is described by a set of four ordinary differential equations in space for liquid mass, vapor mass, mixture energy and mixture momentum (Austregesilo et al., 2012). The CDR1D model has been validated against a large set of experimental data (Wolfert, 1979; Lerchl et al., 2012a), among them several SBLOCA scenarios.

3. Boundary and initial conditions of the investigated scenario and applied accident management measures

The transient starts from nominal power (3850 MW), end-of-cycle core conditions with assumed 12 GWd/tHM average burn-up. The investigated scenario is a small-break loss-of-coolant accident scenario with additional unavailability of components of the emergency core cooling systems (ECCS). The assumptions are made according to the recommendations given by the German reactor safety commission (RSK, 2005):

- A 50 cm^2 leak in the cold leg of loop No. 2 between main coolant pump (MCP) and RPV (leak close to RPV, see Fig. 1),
- Loss of external power supply after turbine trip leads to the stop of the MCPs and with a delay of 40 s to the start of the diesel generators (DG),
- SCRAM is initiated when the primary pressure decreases below 132 bar,
- Secondary cool-down procedure is not available,
- Auxiliary feedwater supply is available,
- Failure and repair of 2 DGs lead to the unavailability of two ECCS (HPIS and LPIS), one out of the two remaining ECCS feeds into the broken loop (loop 2),
- All 8 hydro-accumulators (HAs) are available, cold side HAs are disconnected 500 s after the emergency preparation signal,
- All transients are calculated till failure of RPV or till 16 hours (when a more or less stable state has been reached).

Furthermore, a failure of the switch to sump injection after the depletion of the flooding pools is assumed. This can be caused e.g. if no water is accumulated in the reactor sump due to a postulated leakage, if there is a malfunction of the necessary valve actions or a failure of the sump suction lines. This additional assumption leads to a severe accident scenario, which is investigated in this paper. The evolution of the scenario without any further measures is described in section 4.

For the application of MPI to the primary circuit, it is assumed that a mobile fire pump system is available at the plant and can be connected to one of the emergency core cooling pipes. To the author's knowledge, mobile pump feed connectors are available for injection to secondary side in the current plant design. No such connection points are currently available for injection to primary side. To carry out the proposed accident measure, a modification of the plant design is needed. However, the ECCS pipes connect the flooding pools, located in the annulus, with the primary circuit. The HPIS as well as the LPIS are also located in the annulus. Thus, one option may be a connection of the mobile fire pump system in parallel to the ECCS pumps. Detailed investigations about how the connection can be technically designed are outside the scope of the paper. A mobile fire pump system similar to systems which can be found on the market is used with a maximum pump head of 16.5 bar and a maximum flow rate of 39 kg/s (Albert Ziegler GmbH, 2014). The applied pump characteristic is given in (Tusheva et al., 2014).

For the current scenario, possible coolant reservoirs are the two un-used flooding pools (2 x 450 t of borated water at 30 °C, the other two pools are already emptied during the first part of the transient by the active ECCS). If the pump injects at its maximum flow rate of 39 kg/s this amount will last for approx. 6½ hours. As the investigated transients are longer, it is assumed, that the flooding pools can be refilled with borated water or that additional borated water can be supplied. For the current simulation, unlimited borated coolant supply is assumed for the mobile pump injection (boron concentration 2200 ppm).

Technically, the MPI is implemented in the model as a FILL-object (boundary condition with a given pressure dependent mass flow rate, enthalpy and boron concentration) as shown in Fig. 1. Two possible connection points are discussed in the paper: connection to the cold leg and connection to the hot leg of the single loop. In case of cold leg injection, the injection is directly to the affected leg and partial loss of the injected coolant directly through the leak might occur. However, for the currently selected configuration (leak at loop center elevation, 3 o'clock position), the injected sub-cooled liquid can flow along the lower edge of the pipe to the RPV inlet. In general, the leak may be located on the lower edge of the pipe, which would make injection through this loop impossible. However, a leak location detection system can be used at the plant and consequently the mobile pump should be connected to a non-affected loop. To investigate such a configuration, the current model needs to be extended, with simulation of four individual loops instead of one single loop and one triple loop, which is out of the scope of the current paper.

PSD as additional accident measure is applied by full opening of the pressurizer relief valve and both safety valves.

4. Results of the calculated base scenario without AMM

The investigated base SBLOCA case without application of AMM is described in this section. The key parameters are plotted in the Figures 2–8 (case indicated by "No AMM"). The SBLOCA is started with opening of the leak at t = 1.0 s. The maximum leak flow rate found approximately 1.2 seconds after leak opening is about 580 kg/s. Due to discharge of liquid through the leak, the primary pressure drops and the signal $p_{primary} < 132$ bar leads to reactor SCRAM at t = 22.7 s and turbine trip. The switch to external power supply is assumed to fail for the investigated scenario. Consequently, the MCPs stop and the diesel generators start with a time delay of 40 s.

The pressure is reduced to saturation pressure (≈ 91 bar) within the first 70 s after the leak opening (Fig. 2), while the leak mass flow rate is reduced to about 50 % of its initial peak mass flow rate.

In a Konvoi power plant, as soon as the signal $p_{primary} < 132$ bar is raised, the secondary cool-down will be activated, which leads to a secondary side pressure reduction (following the saturation curve with a temperature reduction of 100 K/h until 2 bars are reached). This procedure is an efficient measure to remove the decay heat from the primary side and in case the auxiliary feedwater supply is available, the power removal can be kept for long term. Furthermore, the primary pressure is also reduced, which leads to reduction of the leak mass flow rate. Consequently, the core can be kept covered with water for long term (at least for 8 hours as shown in (Jobst et al., 2017a)). For the current scenario, the cool-down procedure is not available and the secondary pressure remains at higher level. According to the assumptions made, two out of four ECC trains are available and the HPIS starts to inject at 67 s into the transient. The leak mass loss is compensated by the HPIS injection, the RPV level is kept approximately at the hot leg elevation and the reactor core is covered by water (Fig. 3). However, the 50 cm^2 leak is large enough, that the primary pressure continuously decreases (Fig. 2) until 26 bar is reached at 44 minutes into the transient and the hot leg accumulators start to inject (the cold leg accumulators are already isolated). With further pressure reduction down to 11 bar, the LPIS starts to inject from 1 h 20 min on. The RPV collapsed level already exceeds 0.375 m (top edge of main coolant pipes) and continues to rise. At approx. 1 h 31 min, a large amount of sub-cooled water (80–100 °C) flows to the pressurizer, which was filled with superheated steam before (320 °C). Due to enhanced condensation the pressure drops to approximately 5 bar (Fig. 2), which leads to further injection by HA and LPIS. The HA level drops below 1.65 m and raises the signal for hot side HA isolation at 1 h 32 min. Furthermore, the flooding pools also reach low level. According to

the designed procedures, the ECCS should switch to sump injection. In the current scenario, failure of this switch is assumed. From that moment on, all active ECCS injection is stopped (1 h 32 min).

After the active and passive safety injection systems have stopped working, the primary side pressure increases up to 26 bar due to steam generation in the core and it takes almost 2 hours to relieve the pressure again to values below 10 bar (Fig. 2). This increased pressure leads to an increase in the leak mass flow rate and the RPV level continuously decreases and the core becomes uncovered. The core starts to heat up, a core exit temperature (CET) of 400 °C is reached approximately 3 hours after the initiating event. The severe accident criterion (CET > 650 °C (Loeffler et al., 2012; Vayssier, 2012)) is reached only 19 minutes later. Even before the SAMG signal is activated, the first hydrogen is generated due to zircaloy oxidation, but oxidation rates are low and it takes about 30 minutes to generate a hydrogen amount greater than 10 kg (3 hours 31 min, Fig. 7).

Without any countermeasures, the calculation predicts the first melting of control rods at approximately 3 h 20 min after leak opening, followed by the release of fission products and the melting of the fuel rods. Approximately 3 h 50 min after the beginning of the transient, the total amount of molten ceramics has reached 10 tons. At that time, the total amount of molten material exceeds 35 tons, which is defined as initiation criterion for melt relocation to the lower plenum. As described in section 3 of part I, the formation of a homogenous molten pool is assumed which is covered by a water layer. After the first relocation, a molten pool with a height of approximately 0.8 m and a volume of 4 m^3 is formed. Due to the high heat transfer from the molten pool to the LP coolant (maximum 11 MW) this water layer is completely evaporated approximately 100 minutes after the melt relocation. The heat load on the vessel wall leads to an increase of the vessel wall temperature (see the maximum of the central wall temperature TWCMAX plotted in Fig. 8). The ATHLET-CD simulation predicts the failure of the RPV (plastic rupture) approximately 5 h 50 min after the initiation of the event.

5. Results of the calculated scenario with application of AMM

5.1. Injection by mobile fire pump system connected to cold leg

As stated in section 4, at approximately one and a half hours into the transient, the flooding pools connected to the two available ECC trains are depleted, and hot leg accumulators are at low level. The switch to sump injection fails and from that moment on, it is assumed that no active or passive injection is available from any of the regular ECC systems. As a result, during the next one and a half hours, the coolant in the primary circuit is heated up and partly discharged through the leak, so that core uncovery cannot be avoided and the core starts to heat up and reaches 400 °C at 3 hours into the transient. With additional delay, the core will start to melt.

To avoid further core heat-up, the mobile pump system is connected to one of the cold legs and starts to inject borated water. The effectiveness of the MPI is investigated for a variety of pump activation criteria at different core states. For the first case, it is assumed, that the pump can be activated shortly after detection of CET above 400 °C. That means that the mobile pump system is connected to the primary circuit within 3 hours after beginning of the transient (1½ hours after stop/failure of the active ECCS). A short delay of two minutes (from detection of 400 °C till pump activation) is assumed, taking into account the needed time for pump run-up. Alternative simulations were carried out, with the assumption, that the pump can be activated with some additional delay, when the core is already at elevated temperatures or has experienced partial core melt (m_{melt} > 1 t, … 100 t). For this first set of simulations, the selected pump activation criteria are shown in Table 1 (simulation set #1). The corresponding delay after detection of CET > 400 °C is also given in this table. Some of the simulations showed unintended code termination due to code errors or unreasonable results (see details given in (Jobst et al., 2016; Jobst et al., 2017a; Kliem et al., 2017)).

The Figures 2(a)–8(a) show selected results of the first set of simulations (only cases without code errors are shown in the figures). The simulations are grouped according to the qualitative evolution of the transient and colors are used to distinguish between the groups. The colors in the plots have the following meaning:

- Magenta: Base case without any AMM (core melt with relocation to lower head and RPV failure),
- Blue: Core melt with release of fission products, but no relocation of core material to lower head,
- Orange: Core melt with relocation of corium to the lower head, but no RPV failure (due to implemented plastic rupture criterion, see discussion in section 2),
- Red: Core melt with relocation of corium to lower head, with RPV failure.

The same color groups are used for subsequent plots (simulation set #2, figures in the following sections), where additional groups can be identified:

- Green: No release of fission products, no absorber melting,
- Dark-olive green: No release of fission products, but melting of absorber,

- Brown: Base case with PSD at 400 °C and without MPI (core melt with relocation to lower head and RPV failure).

Furthermore, the simulations with RPV failure are limited in time till its occurrence (indicated by "X" in the figures).

If the pump is activated at CET > 400 °C (3 h 3 min), the primary pressure is above 20 bar (see Fig. 2(a)) and no injection is possible until approximately 3 h 20 min when the primary pressure has dropped again below 16.5 bar, due to the reduction of coolant level in the core and reduced steam production. This is accompanied by an increase of CET to 650 °C. From that time point on, the pump can inject, but due to the increased steam production, the pressure increases again and injection is interrupted several times. Therefore, it takes more than 3 hours to increase the RPV level till RPVMIN3 (0.15 m below center of hot leg, Fig. 3(a)). During the reflooding period a maximum cladding temperature of 1180 °C (1190 °C fuel temperature) is observed at 3 h 38 min (Fig. 4(a)). Due to this high cladding temperature, the oxidation process already starts and failure of the cladding with release of fission products from the core to primary circuit is predicted. However, the amount of generated hydrogen and released fission products is several orders of magnitude less than for the case without AMM, described above: H_2 production is reduced by a factor of 145 to approx. 4.6 kg, FP release is reduced by a factor of approx. 300 to $4.4 \cdot 10^{17}$ Bq. The observed peak cladding temperature is much less than the fuel melting temperature (2600 K).

The case with pump activation delayed till detection of 650 °C CET (plus two additional minutes for pump run-up, i.e. pump activation at 3 h 22 min) develops in a very similar way. As described above, at that time the pressure already dropped below 16.5 bar and the pump can start to inject immediately. However, due to this short delay of 1 min in beginning of injection in combination with enhanced oxidation processes, the maximum observed cladding temperature increases by 200 K to 1390 °C (1400 °C fuel temperature, see Fig. 4(a)). The amount of released H_2 is already almost doubled to 8.7 kg.

Additional 5 minutes later, already 1 t of molten absorber material is observed. If the pump could be activated at that moment, the partial core melt is cooled down and the core can be transferred into a long-time coolable state. However, due to the slow reflooding process, cladding temperature reaches 2215 °C, which leads to the melting of the fuel rods. The final amount of released FP is already increased to $1.95 \cdot 10^{18}$ Bq (increased by a factor of four compared to the earlier injection started at 650 °C CET) and the final amount of released H_2 is increased to 100 kg.

Our model shows that pump activation with further delay can cool the core and prevent relocation to the lower head, if the pump is activated not later than 45 minutes after detection of 400 °C CET. At that moment, already 18 t (11 %) of the core are molten and partial relocation has occurred within the core. The reflooding of the vessel is still slow and further core material melts, but the core melting can be stopped with maximum of 32 t molten material, which is lower than the user-provided set point for start of relocation to the lower head (35 t). For cases with further delay in start of the MPI, the 35 t set point is reached. This leads to the formation of a molten pool in the lower head, which is covered by coolant. Prior to the relocation of core material, the amount of remaining coolant in the LH is around 18 t. Even if the pump has not been started yet, this coolant is enough to cool the molten pool for more than one hour and in all cases until the MPI activation. A maximum void in LH of 0.15 is found for the case with the latest pump activation at 100 t core melt mass (60 % of the core). For the investigated scenario with relatively fast core degradation, the higher the amount of corium relocated to LH the higher is the LH heat source and the higher is the maximum observed wall temperature. For cases with pump activation not later than 4 h 10 min (at 80 t core melt, 69 minutes after CET > 400 °C), the maximum calculated central wall temperature TWCMAX is 1200 °C (see Fig. 8(a) at approx. 6 h 30 min). For such conditions the plastic rupture model predicts no failure of the vessel. According to the Larson-Miller approach, a creep rupture is predicted at 71 hours (beyond the end of simulation). The implemented Larson-Miller calculation procedure assumes conservatively that the maximum load is maintained infinitely after its first occurrence. As could be seen from Fig. 8(a), TWCMAX is reduced down to 1050 °C till 16 hours (and is expected to be further reduced due to decay power reduction), which also reduces the creep rates and the time till creep rupture will be further extended. However, the peak TWCMAX is only 25 K below 1500 K (the implemented melting temperature, at which, according to the plastic rupture model, rupture will occur anyway), and for the observed conditions, the ratio between stress and ultimate stress is around 0.75. On the other hand, if one looks at the whole radial wall temperature profile, 50 % of the wall (74 mm) are at temperatures lower than 1200 °C (maximum surface temperature 800 °C), and the primary pressure is relatively low at approximately 1.0 MPa. As stated in section 2, creep processes are only significant for high temperatures and pressures above 1.0 MPa. As the pressure in the described cases is close to this value, further investigations are needed, to assess if creep rupture really plays a significant role. However, for the late start of the MPI, high uncertainty about the evolution of the transient has to be taken into account and therefore the current result obtained from a single deterministic (best estimate) calculation should be treated with caution. For cases with earlier pump activation, not later than 3 h 53 min (at 40 t core melt, 52 minutes after CET > 400 °C), TWCMAX is around 980 °C, i.e. 250 K below 1500 K. For such

conditions the calculated maximum ratio between stress and ultimate stress is less than 0.02 and no plastic rupture will occur. The Larson-Miller approach predicts for these conditions RPV failure after more than 2 years (again assuming infinitely lasting maximum load despite the fact that decay heat is reduced significantly).

As stated above, the mobile pump system cannot start to inject immediately after CET > 400 °C due to the fact that the primary pressure is higher than the maximum pump head. Therefore, primary side depressurization (PSD) is applied as additional measure to reduce the primary pressure below the pump head. According to the scheme for German PWRs (Fig. 2 presented in (Wilhelm et al., xxxx)), PSD should be applied if CET reaches 400 °C (latest criterion). We follow this procedure here and apply PSD at 400 °C for the second set of simulations. One simulation was performed with PSD only; in the second one MPI is also activated when CET reaches 400 °C (again with additional delay of two minutes for pump run-up). As above, similar simulations with delayed pump activation were carried out. The right part of Table 1 shows a complete list of the applied activation criteria. The Figures 2(b)–8(b) depict selected results of this second set of simulations. Due to the code errors mentioned above, not all simulations with the given pump activation criteria as in the first set could be included into the comparison of the results. Therefore, simulations with similar activation criteria were tested. Nevertheless, in the melt mass range between 1 t and 15 t, all simulations terminated shortly after start of mobile injection. As could be seen from the code results depicted in Fig. 5(b), mobile pump activation at 1 t melt mass (3 h 21 min) is the latest possible activation, for which the core melt progression can be stopped. Finally for this case a corium mass of 7.2 t is observed. If the pump is activated at a melt mass of 15 t (3 h 37 min) or beyond, the melt progression will continue until the melt masses reaches 35 t, which is the set point for corium relocation to the lower head. With the current code results, no statement can be made for MPI start in the melt mass range between 1 t and 15 t (i.e. between 3 h 21 min and 3 h 37 min). Conservatively, one has to conclude for this range, that the melt progression cannot be stopped and relocation to the lower head will occur.

In general, the application of PSD at 400 °C CET (see brown curves in Figures 2(b)–8(b)) leads to a reduction of the primary pressure from 24 bar to the maximum pump head of mobile pump within 2 minutes and further pressure reduction afterwards (Fig. 2(b)). This is accompanied by a fast drop of the RPV collapsed level (within 3 minutes below the lower edge of the active core, Fig. 3(b)). If the mobile pump cannot be activated, the increased loss of coolant through the pressurizer valves leads to earlier occurrence of the following processes like the start of core melt (Fig. 5(b)), release of fission products (Fig. 6(b)) and H_2 release (Fig. 7(b)) and ½ hour earlier vessel failure (see Table 1).

If the pump can be activated after PSD, the injection rates are higher and vessel reflooding is faster compared to the cases without PSD (compare Fig. 3(b) vs. Fig. 3(a) and timings given in Table 1). For the case with pump activation at 400 °C CET, the reflooding process in combination with PSD takes only 37 minutes, instead of more than 3 hours without PSD. Due to the faster reflooding, the observed maximum cladding and maximum fuel temperatures do not exceed 625 °C (Fig. 4(b)). Therefore no cladding failure and no fission product release (Fig. 6(b)) is predicted by the code for this case. This leads to the conclusion, that if MPI is considered as AMM for the investigated SBLOCA, the release of fission products can only be avoided, if early MPI is combined with additional PSD. If there is an additional delay between PSD and pump activation (CET > 650 °C or beyond), failure of the fuel rods and fission product release are predicted. Furthermore, for start of MPI at CET > 650 °C, the simulations show a more severe progression of the accident compared to cases without PSD, in respect to hydrogen generation and release of fission products. See section 5.4 for details.

Table 1. Applied pump activation criteria for cold leg injection and selected timings.

MPI to cold leg; Pump activation could be established at	Without PSD, Simulation set #1								With PSD at CET > 400 °C, Simulation set #2							
	Pump activation		Duration till RPV level > MIN3	FP release	Start of core melt (absorber)	Reloca-tion to LH	RPV failure		Pump activation		Duration till RPV level > MIN3	FP release	Start of core melt (absorber)	Reloca-tion to LH	RPV failure	
	Time	Delay after CET > 400°C					Plastic rupture model	Larson-Miller	Time	Delay after CET > 400°C					Plastic rupture model	Larson-Miller
	[h:min]	[min]	[min]	[h:min]	[h:min]	[h:min]	[h:min]	[h]	[h:min]	[min]	[min]	[h:min]	[h:min]	[h:min]	[h:min]	[h]
No pump injection	n/a	n/a	n/a	3:26	3:23	3:52	5:53	19.5	n/a	n/a	n/a	3:17	3:16	3:43	5:19	19.5
CET > 400 °C	3:03	2	202	3:28	3:24	-	-	-	3:03	2	37	-	-	-	-	-
CET > 650 °C	3:22	21	168	3:27	3:23	-	-	-	3:16	15	42	3:18	3:16	-	-	-
m_{melt} > 1 t	3:27	26	184	3:26	3:23	-	-	-	3:21	20	49	3:17	3:16	-	-	-
m_{melt} > 5 t	3:36	35	145	3:26	3:23	-	-	-	No results due to code termination							
m_{melt} > 10 t	3:38	37	109	3:26	3:23	-	-	-	No results due to code termination							
m_{melt} > 15 t	No results due to code termination								3:37	36	56	3:17	3:16	3:45	-	$2.25 \cdot 10^6$
m_{melt} > 18 t	3:46	45	97	3:26	3:23	-	-	-	3:39	38	67	3:17	3:16	3:43	-	$6.43 \cdot 10^5$
m_{melt} > 20 t	No results due to code termination								No results due to code termination							
m_{melt} > 22 t	3:48	47	105	3:26	3:23	3:52	-	$1.34 \cdot 10^5$	3:41	40	58	3:17	3:16	3:43	-	17100
m_{melt} > 25 t	No results due to code termination								No results due to code termination							
m_{melt} > 30 t	3:50	49	104	3:26	3:23	3:51	-	$1.32 \cdot 10^5$	No results due to code termination							
m_{melt} > 35 t	No results due to code termination								3:43	42	57	3:17	3:16	3:43	-	3030
m_{melt} > 40 t	3:53	52	125	3:26	3:23	3:52	-	18200	3:44	43	57	3:17	3:16	3:43	-	3530
m_{melt} > 50 t	3:56	55	64	3:26	3:23	3:52	-	173	3:46	45	60	3:17	3:16	3:43	-	1450
m_{melt} > 60 t	3:59	58	59	3:26	3:23	3:52	-	133	3:52	51	49	3:17	3:16	3:43	5:26	19
m_{melt} > 70 t	4:01	60	60	3:26	3:23	3:52	-	115	3:56	55	51	3:17	3:16	3:43	5:26	20
m_{melt} > 80 t	4:10	69	56	3:26	3:23	3:52	-	71	3:57	56	50	3:17	3:16	3:43	5:27	21
m_{melt} > 90 t	4:18	77	55	3:26	3:23	3:52	5:45	32	4:20	79	53	3:17	3:16	3:43	5:31	23
m_{melt} > 100 t	4:34	93	63	3:26	3:23	3:52	5:48	37	4:34	93	56	3:17	3:16	3:43	5:26	15

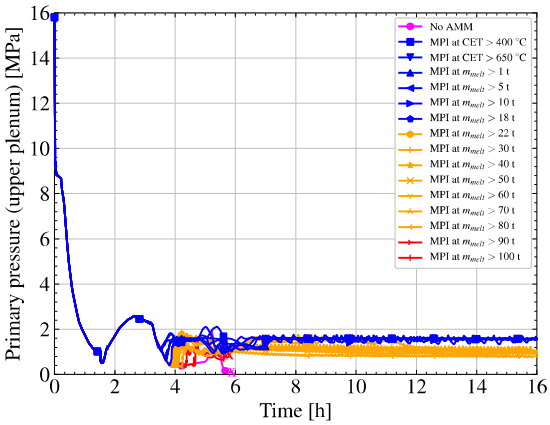

(a) Without PSD.

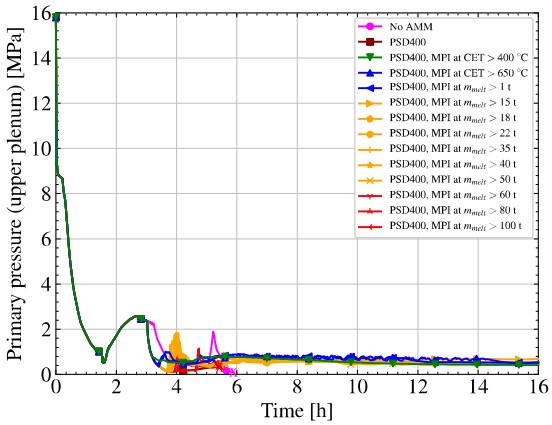

(b) With PSD applied at CET > 400 °C.

Fig. 2. Mobile pump injection to cold leg. Primary pressure.

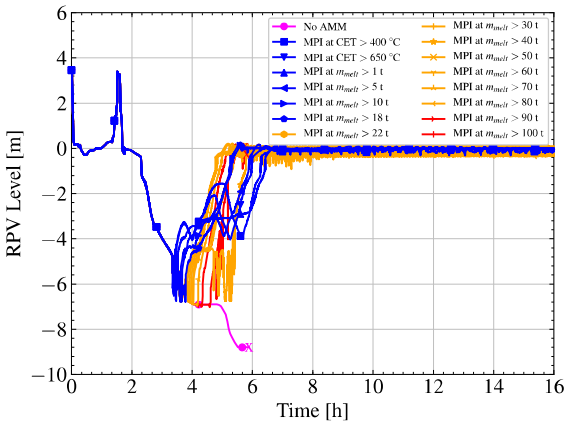

(a) Without PSD.

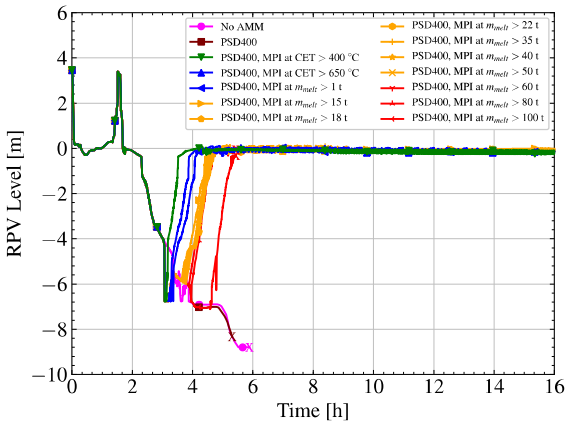

(b) With PSD applied at CET > 400 °C.

Fig. 3. MPI to cold leg. RPV collapsed level.

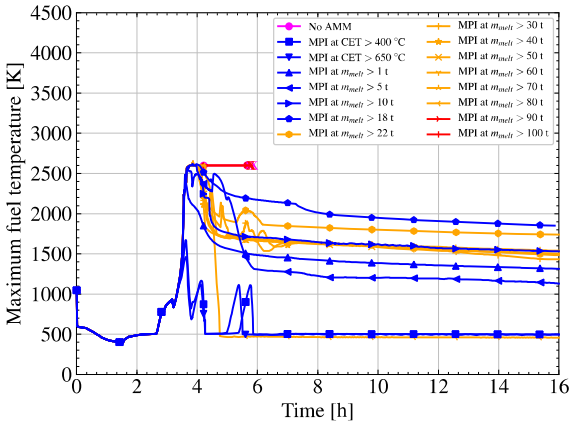

(a) Without PSD.

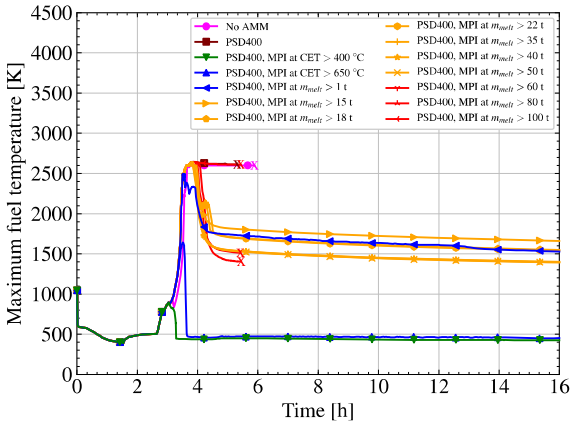

(b) With PSD applied at CET > 400 °C.

Fig. 4. MPI to cold leg. Maximum fuel temperature.

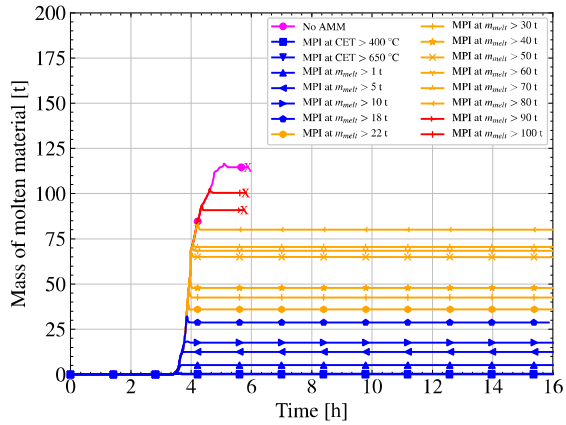

(a) Without PSD.

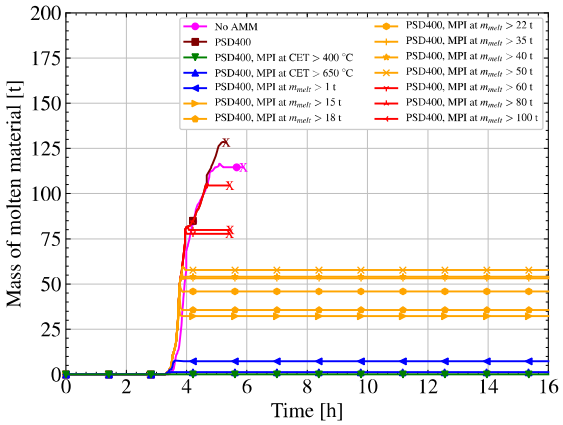

(b) With PSD applied at CET > 400 °C.

Fig. 5. MPI to cold leg. Mass of molten core material.

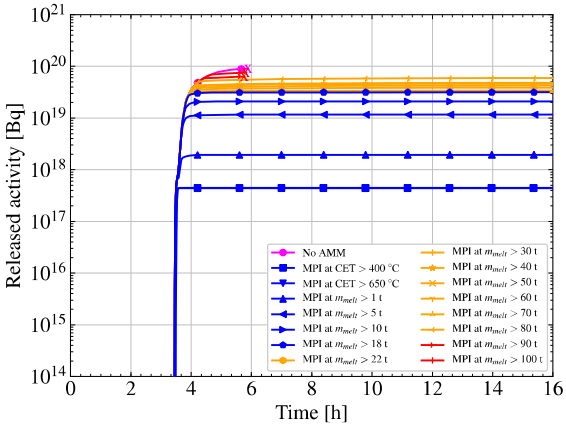

(a) Without PSD.

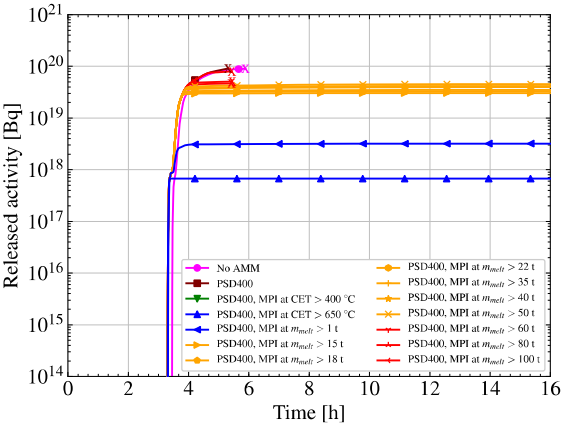

(b) With PSD applied at CET > 400 °C.

Fig. 6. MPI to cold leg. Released activity (from the core to RPV).

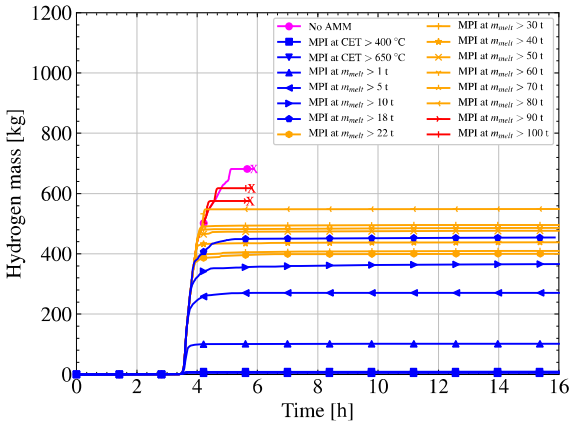

(a) Without PSD.

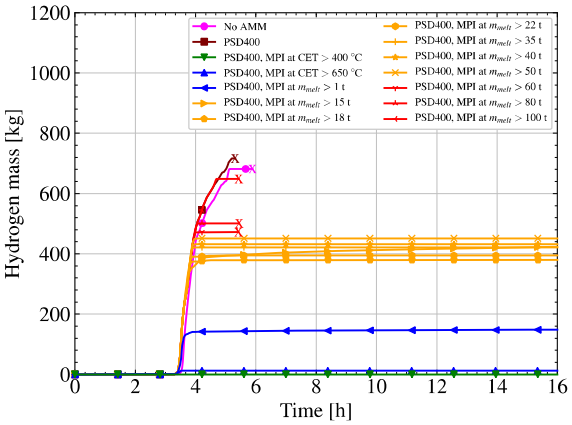

(b) With PSD applied at CET > 400 °C.

Fig. 7. MPI to cold leg. Mass of released hydrogen.

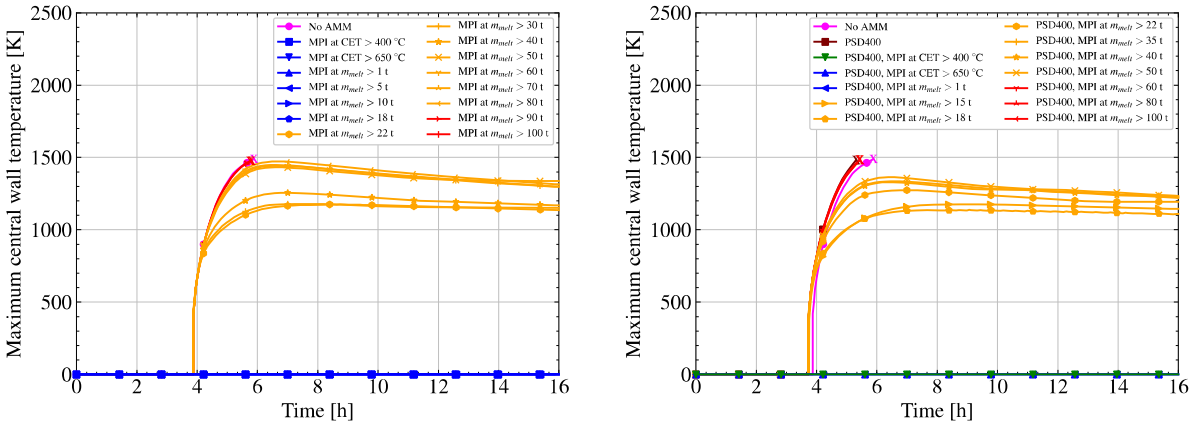

(a) Without PSD. (b) With PSD applied at CET > 400 °C.

Fig. 8. MPI to cold leg. Maximum central wall temperature in lower head.

5.2. Injection by mobile fire pump system connected to hot leg

Alternatively to the cold leg injection, MPI to the hot leg was investigated. The hot leg of loop No. 2 (single loop) was selected as connection point. Similar to the cold leg injection case, it was assumed that the mobile pump can be connected to the ECCS injection lines. In German Konvoi reactor, the coolant injected to the hot leg is directed to the upper plenum by application of a scoop (Hutze, see e.g. (Lerchl et al., 2012b)), which could increase the effectiveness of the injection. The cold coolant (taken from the remaining two flooding pools) is directed to the upper plenum and injected to the outer most region of the core (core channel 6). From this channel the coolant is distributed to the inner core channels by cross connections.

Again two sets of simulations were performed. In the first set with MPI as single AMM (simulation set #3), the MPI onset was again varied in a wide range from early accident conditions (CET > 400 °C) till more severe conditions later during the transient at elevated CET (650 °C) as well as already partly molten core (m_{melt} > 1 t, … 100 t, see left part of Table 2). In the second set, one simulation with PSD as single AMM was performed and additional simulations with combined PSD initiated at 400 °C CET and MPI initiated at varied core conditions (set #4, see right part of Table 2). Again, cases with code errors are excluded from the comparison. Selected key parameters are shown in the Figures 9 to 12. The chosen plot colors again indicate how the transient evolves qualitatively (see color key given in section 5.1).

Without PSD, RPV reflooding by MPI through the hot leg takes longer time than the cold leg injection (compare Fig. 9(a) with Fig. 3(a)). This is due to the fact that coolant injected to the hot leg is directed to the hottest part of the core (upper part of the core), which leads to an increased steam production and an increase of the pressure compared to the cold leg injection cases. Furthermore, the coolant injection is reduced by the counter current flow in the hot leg. The duration till the collapsed level reaches the elevation of the hot legs (RPVMIN3) compared to the cold leg injection cases is increased by values ranging from 20 % (early start of injection) till a factor of three (late start of injection). If MPI is started at CET equal to 400 °C or 650 °C, the injection is interrupted later during the transient for more than 1 hour. For these cases, until approximately 7 h 20 min, the level in the primary system is increased till the leak in cold leg is partly covered by liquid. Consequently, liquid is discharged through the leak which leads to a reduction of steam discharge and an increase of the primary pressure which exceeds the maximum pump head of the mobile pump. The temporary MPI interruption leads to a decrease of RPV level (Fig. 9(a)), till the reduced steam production again lowers the primary pressure and restores MPI. Afterwards intermittent injection is observed. In case of already higher fission product release (with therefore reduced core power, see the case with start of the MPI at 5 t melt mass in Fig. 9(a)), a similar behavior of the leak discharge is found, but due to the lower core power, less steam is produced and the intermittent MPI occurs earlier (no long term interruption). Cases with material already relocated to LH show higher release of FP (Fig. 11(a)) and partial heat removal through the vessel wall, and therefore less remaining power to heat the coolant (from remaining core and LH molten pool). For these cases a nearly complete coverage of the leak with liquid is observed (Fig. 9(a)). The heat is removed mainly through the leak by discharge of heated liquid coolant. Due to the much slower reflooding process, the MPI through hot leg leads to more severe final conditions than injection through cold leg (see also summary discussion in section 5.4).

If PSD at 400 °C CET is applied as a second measure and MPI could be established immediately or with further delay (Fig. 9(b)–Fig. 12(b)), the RPV reflooding is completed in comparably short times than it was found for the cold leg MPI cases. However, the coolant is injected directly to the upper part of the core and

therefore shows a better effect in cooling of the hottest structures. According to our simulations, MPI activation at 3 h 16 min prevents FP release in case of hot leg injection, while this is not the case for cold leg injection. Further positive effects (lower H_2 release due to the fast cool down of the hottest structures) can be seen prior to 3 h 30 min, later on more negative effects of hot leg injection are observed (higher H_2 release due to slower vessel reflooding for late MPI and continues injection of coolant from top of the core, see summary section 5.4).

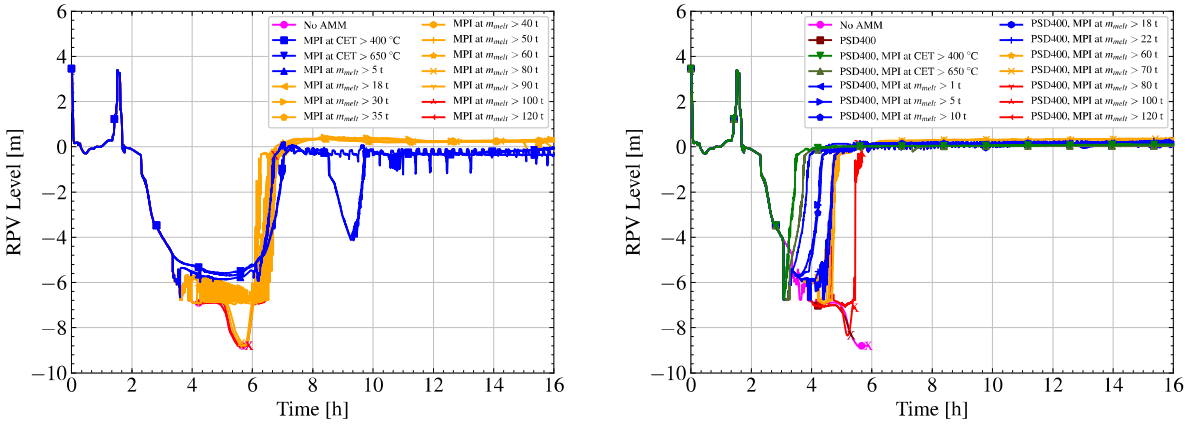

(a) Without PSD. (b) With PSD applied at CET > 400 °C.

Fig. 9. MPI to hot leg. RPV collapsed level.

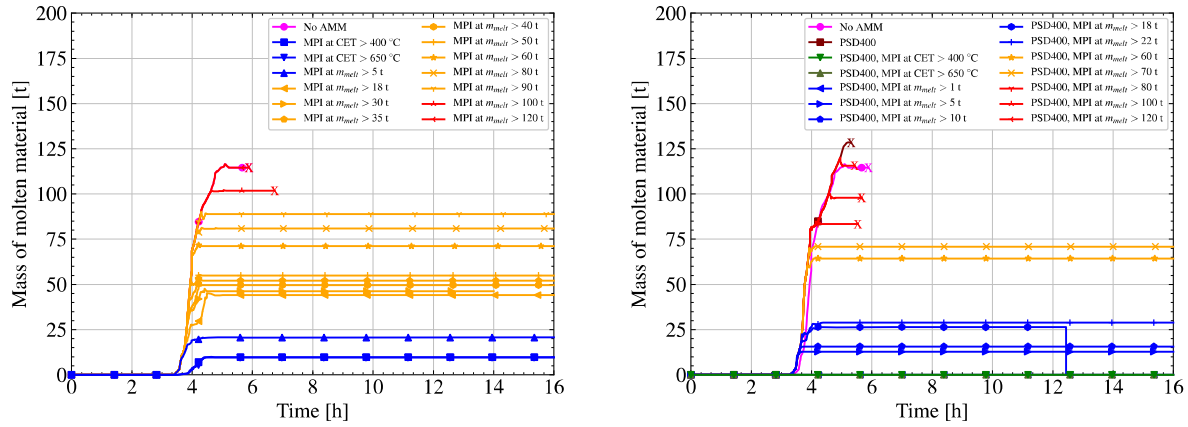

(a) Without PSD. (b) With PSD applied at CET > 400 °C.

Fig. 10. MPI to hot leg. Mass of molten core material.

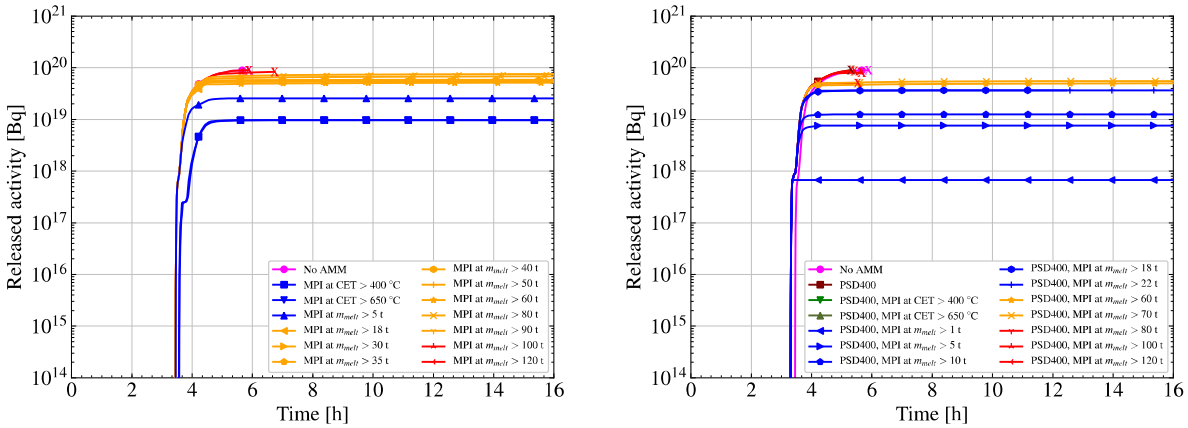

(a) Without PSD. (b) With PSD applied at CET > 400 °C.

Fig. 11. MPI to hot leg. Released activity (from the core to RPV).

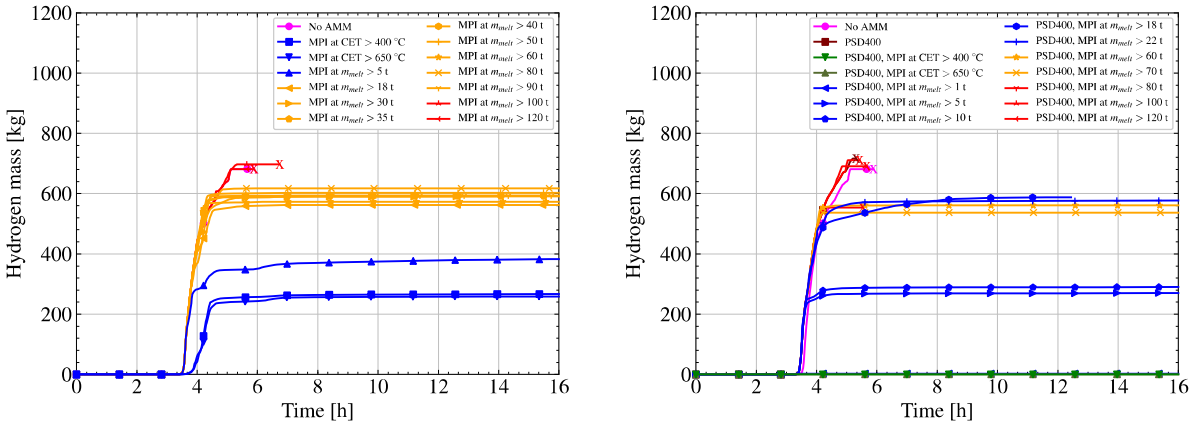

(a) Without PSD.

(b) With PSD applied at CET > 400 °C.

Fig. 12. MPI to hot leg. Mass of released hydrogen.

Table 2. Applied pump activation criteria for hot leg injection and selected timings.

MPI to hot leg; Pump activation could be established at	Without PSD, Simulation set #3								With PSD at CET > 400 °C, Simulation set #4							
	Pump activation		Duration till RPV level > MIN3	FP release	Start of core melt (absorber)	Reloca-tion to LH	RPV failure		Pump activation		Duration till RPV level > MIN3	FP release	Start of core melt (absorber)	Reloca-tion to LH	RPV failure	
	Time	Delay after CET > 400°C					Plastic rupture model	Larson-Miller	Time	Delay after CET > 400°C					Plastic rupture model	Larson-Miller
	[h:min]	[min]	[min]	[h:min]	[h:min]	[h:min]	[h:min]	[h]	[h:min]	[min]	[min]	[h:min]	[h:min]	[h:min]	[h:min]	[h]
No pump injection	n/a	n/a	n/a	3:26	3:23	3:52	5:53	19.5	n/a	n/a	n/a	3:17	3:16	3:43	5:19	19.5
CET > 400 °C	3:03	2	246	3:33	3:26	-	-	-	3:03	2	35	-	-	-	-	-
CET > 650 °C	3:21	20	228	3:33	3:25	-	-	-	3:16	15	37	-	3:16	-	-	-
m_{melt} > 1 t	No results due to code termination								3:20	19	40	3:17	3:16	-	-	-
m_{melt} > 5 t	3:35	34	195	3:26	3:23	-	-	-	3:29	28	62	3:17	3:16	-	-	-
m_{melt} > 10 t	No results due to code termination								3:32	31	58	3:17	3:16	-	-	-
m_{melt} > 15 t	No results due to energy balance error								No results due to code termination							
m_{melt} > 18 t	3:46	45	180	3:26	3:23	4:21	-	$1.94 \cdot 10^6$	3:39	38	73	3:17	3:16	-	-	-
m_{melt} > 20 t	No results due to energy balance error								No results due to code termination							
m_{melt} > 22 t	No results due to energy balance error								3:40	39	72	3:17	3:16	-	-	-
m_{melt} > 25 t	No results due to energy balance error								No results due to code termination							
m_{melt} > 30 t	3:50	49	184	3:26	3:23	3:56	-	$2.10 \cdot 10^6$	No results due to code termination							
m_{melt} > 35 t	3:51	50	172	3:26	3:23	3:52	-	$2.18 \cdot 10^5$	No results due to energy balance error							
m_{melt} > 40 t	3:53	52	177	3:26	3:23	3:52	-	$1.60 \cdot 10^5$	No results due to energy balance error							
m_{melt} > 50 t	3:56	55	172	3:26	3:23	3:52	-	$1.58 \cdot 10^5$	No results due to energy balance error							
m_{melt} > 60 t	3:57	56	162	3:26	3:23	3:52	-	484	3:51	50	60	3:17	3:16	3:43	-	3630
m_{melt} > 70 t	4:01	60	159	3:26	3:23	3:52	-	372	3:55	54	54	3:17	3:16	3:43	-	386
m_{melt} > 80 t	4:09	68	149	3:26	3:23	3:52	-	261	3:56	55	51	3:17	3:16	3:43	5:32	23.2
m_{melt} > 90 t	4:17	76	168	3:26	3:23	3:52	-	133	4:18	77	61	3:17	3:16	3:43	6:00	41.3
m_{melt} > 100 t	4:33	92	158	3:26	3:23	3:52	6:44	56	4:33	92	86	3:17	3:16	3:43	5:40	25.0

5.3. Delayed PSD in combination with immediate injection by the mobile fire pump system

The depressurization of primary side leads to a fast level reduction due to enhanced evaporation and discharge through the pressurizer valves. If PSD is applied at CET > 400 °C (according to the scheme Fig. 2 in part I), but additional time is needed to activate the mobile pump, as it is assumed in the simulation sets #2 and #4, the core is completely uncovered for a certain time until the level could be restored by the MPI. Compared to the case without AMM, the core level is significantly lower for a duration of up to 30 minutes (see Fig. 3(b)). This long duration of low core level may be prevented if PSD is shifted until the mobile pump is also ready to inject. Therefore two additional simulation sets were carried out, set #5 for delayed PSD and immediate activation of the pump injection to the cold leg, and set #6 for delayed PSD and immediate activation of the pump injection to the hot leg. The activation criteria of PSD and MPI were again varied in a wide range, covering a time range of approximately 90 minutes after the detection of CET > 400 °C (see Table 3).

Key parameters are shown in the Figs. 13–16. Many of the simulations with cold leg injection were terminated shortly after start of injection due to code errors. Therefore very limited results could be obtained especially in the interesting intermediate core melt range (these simulations have been excluded from the assessment of the results and not shown in the plots). However, for hot leg injection, most simulations could be finished successfully.

Both sets show comparable durations from the start of the MPI till the RPV level reaches the elevation of the hot leg (RPVMIN3), ranging from 35 minutes in case of early injection till approx. 75 minutes for later injection. In case of hot leg MPI, the effect of direct cooling of the hottest structures is visible. If MPI is activated at latest 20 minutes after CET > 400 °C, no release of FP is predicted in case of hot leg injection. In the case of cold leg injection, FP release can already be observed. The immediate injection by mobile pump to the hot leg also shows the effect, that the melt progression can be stopped very rapidly, even in cases of already high melt masses. For example if the MPI is started at 3 h 50 min (approx. 50 minutes after detection of CET > 400 °C), due to an already reduced pressure (4 bar before the application of AMM), the pump can inject at almost its maximum flow rate (approx. 38 kg/s at the start of MPI) to the upper part of the core, which leads to an enhanced steam production. Due to PSD, the following pressure increase is limited (approx. 12 bar) and the pump can still inject at relatively high flow rates (≈ 27 kg/s). Therefore, a stop of melt progression is predicted within approximately 15 minutes. Similar observations can be made for the other investigated cases (Fig. 14(b)). However, despite the maximum core temperature is significantly reduced below the fuel melting temperature for all cases with injection, it remains above 1800 K for approximately 1 hour and cladding oxidation is still on-going (high H_2 release, Fig. 16(b)).

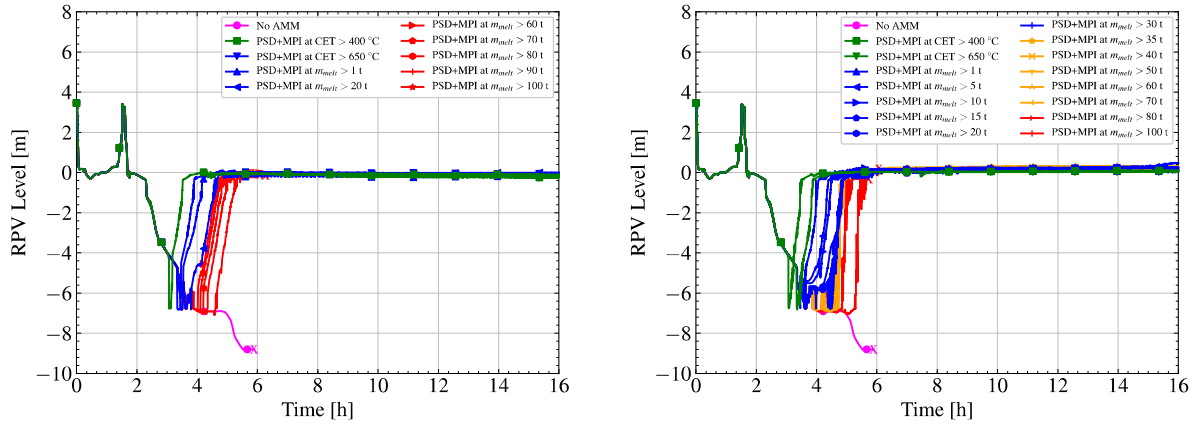

(a) MPI to cold leg.

(b) MPI to hot leg.

Fig. 13. Delayed PSD and MPI. RPV collapsed level.

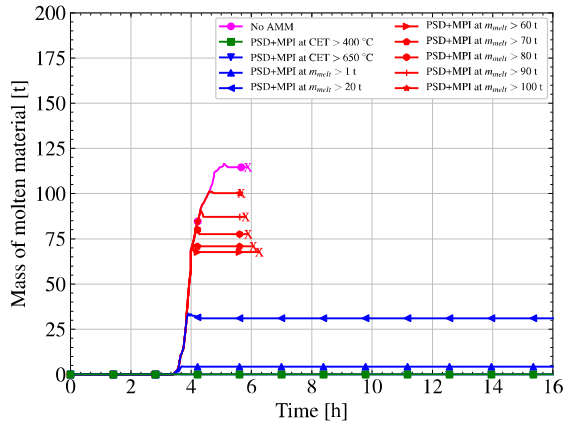

(a) MPI to cold leg.

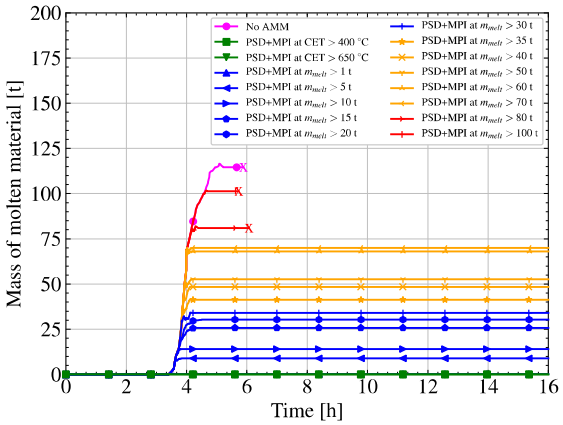

(b) MPI to hot leg.

Fig. 14. Delayed PSD and MPI. Mass of molten core material.

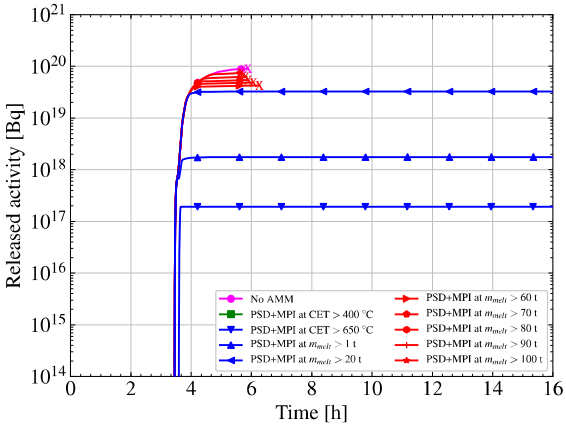

(a) MPI to cold leg.

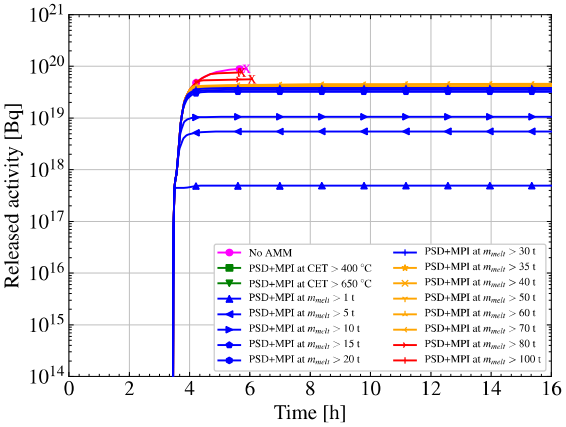

(b) MPI to hot leg.

Fig. 15. Delayed PSD and MPI. Released activity (from the core to RPV).

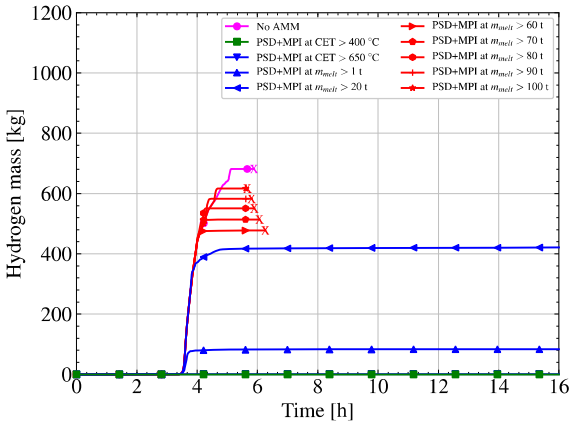

(a) MPI to cold leg.

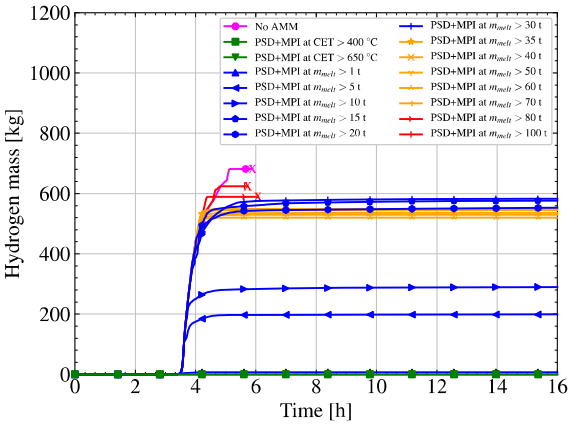

(b) MPI to hot leg.

Fig. 16. Delayed PSD and MPI. Mass of released hydrogen.

Table 3. Applied pump activation criteria for cold leg and hot leg injection and selected timings.

PSD + MPI activated at	Delayed PSD, Injection to cold leg, Simulation set #5								Delayed PSD, Injection to hot leg, Simulation set #6							
	Pump activation		Duration till RPV level > MIN3	FP release	Start of core melt (absorber)	Reloca-tion to LH	RPV failure		Pump activation		Duration till RPV level > MIN3	FP release	Start of core melt (absorber)	Reloca-tion to LH	RPV failure	
	Time	Delay after CET > 400°C					Plastic rupture model	Larson-Miller	Time	Delay after CET > 400°C					Plastic rupture model	Larson-Miller
	[h:min]	[min]	[min]	[h:min]	[h:min]	[h:min]	[h:min]	[h]	[h:min]	[min]	[min]	[h:min]	[h:min]	[h:min]	[h:min]	[h]
No AMM	n/a	n/a	n/a	3:26	3:23	3:52	5:53	19.5	n/a	n/a	n/a	3:26	3:23	3:52	5:53	19.5
CET > 400 °C	3:03	2	37	-	-	-	-	-	3:03	2	35	-	-	-	-	-
CET > 650 °C	3:21	20	36	3:36	3:26	-	-	-	3:21	20	40	-	3:23	-	-	-
m_{melt} > 1 t	3:27	26	49	3:26	3:23	-	-	-	3:27	26	42	3:26	3:23	-	-	-
m_{melt} > 5 t	No results due to code termination								3:35	34	52	3:26	3:23	-	-	-
m_{melt} > 10 t	No results due to code termination								3:38	37	53	3:26	3:23	-	-	-
m_{melt} > 15 t	No results due to code termination								3:44	43	76	3:26	3:23	-	-	-
m_{melt} > 20 t	3:47	46	54	3:26	3:23	-	-	-	3:47	46	70	3:26	3:23	-	-	-
m_{melt} > 25 t	No results due to code termination								3:49	48	74	3:26	3:23	-	-	-
m_{melt} > 30 t	No results due to code termination								3:50	49	67	3:26	3:23	-	-	-
m_{melt} > 35 t	No results due to code termination								3:52	51	69	3:26	3:23	3:52	-	$2.01 \cdot 10^6$
m_{melt} > 40 t	No results due to code termination								3:53	52	67	3:26	3:23	3:52	-	n/a
m_{melt} > 50 t	No results due to code termination								3:56	55	59	3:26	3:23	3:52	-	12900
m_{melt} > 60 t	3:59	58	49	3:26	3:23	3:52	6:16	68	3:59	58	48	3:26	3:23	3:52	-	102
m_{melt} > 70 t	4:01	63	51	3:26	3:23	3:52	6:04	61	4:01	60	51	3:26	3:23	3:52	-	78
m_{melt} > 80 t	4:09	68	55	3:26	3:23	3:52	5:54	46	4:09	68	55	3:26	3:23	3:52	6:04	51
m_{melt} > 90 t	4:17	76	54	3:26	3:23	3:52	5:49	33	4:17	76	61	3:26	3:23	3:52	6:00	41
m_{melt} > 100 t	4:34	93	60	3:26	3:23	3:52	5:40	21	4:34	93	62	3:26	3:23	3:52	5:44	13

5.4. Comparison of all injection cases

The results of all six simulation sets are now summarized in this section. The Figures 17–19 depict several key parameters of the investigated scenario with MPI. On their abscissa, the delay after detection of CET > 400 °C till the activation of MPI is given. The left most plotted points are given for a delay of 2 minutes after CET > 400 °C, taking into account 2 minutes time for mobile pump run-up. The subsequent data points correspond to later core states at higher CET or with already partly molten core. The vertical dashed lines indicate important events which occur in the SBLOCA scenario without any AMM. From these events, the core state at the beginning of MPI can be identified. Fig. 17 shows the duration of the vessel reflooding after the activation of the MPI. As discussed above, PSD reduces the needed time significantly due to the increased pump injection rates. Without PSD, hot leg injection is less effective and the reflooding of the RPV takes much longer. With PSD, the predicted times for reflooding are comparable for cold leg and hot leg injection, with slightly longer times for hot leg injection if it is started between 30 and 50 minutes after CET > 400 °C.

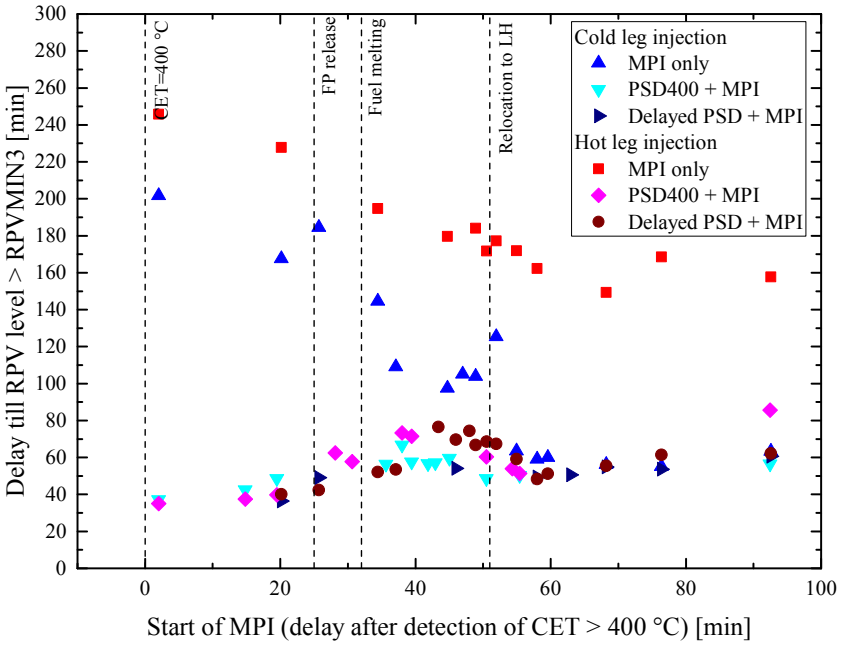

Fig. 17. Delay after activation of the MPI until the RPV collapsed level reaches the elevation of the hot leg (RPVMIN3) depending on the start of the MPI (in terms of delay after detection of CET > 400 °C), point of injection and additional application of PSD.

Fig. 18 summarizes the release of activity from the fuel rods to the primary circuit coolant till 16 hours, which is calculated for all cases with MPI. The dashed horizontal lines indicate the values of the SBLOCA case without AMM. For all simulated cases with pump injection, a reduction of the FP release is predicted. PSD is needed to prevent FP release for the early start of injection at CET > 400 °C. For later start of injection at CET > 650 °C, prevention of FP release is only possible if hot leg injection is combined with a delayed PSD. Therefore, this injection strategy provides the longest time margins to prevent FP release. For later start of the MPI, the releases predicted for this injection strategy show the lowest values and therefore it would be the preferred strategy. Till approx. 40 minutes after CET > 400 °C, significant lower releases, compared to the other injection strategies, are predicted. Later on, this strategy still shows lower release compared to a strategy with early PSD at CET > 400 °C or hot leg injection without PSD. Compared to cold leg injection without PSD or cold leg injection with delayed PSD, the preferred injection strategy does not show significant deviations in activity release.

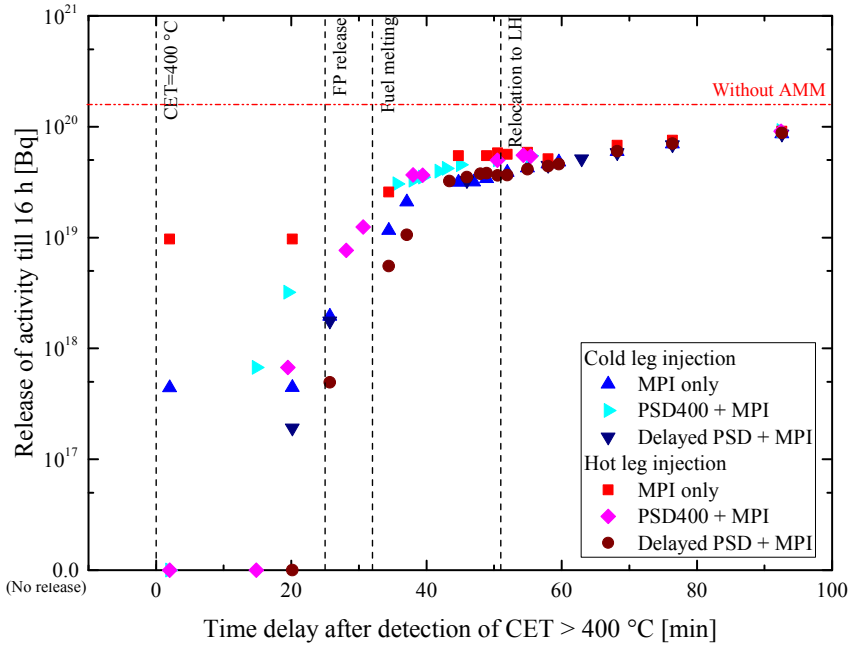

Fig. 18. Releases of activity (from the fuel rods to the primary circuit) depending on the start of the MPI (in terms of delay after detection of CET > 400 °C), point of injection and additional application of PSD.

Fig. 19 summarizes the total amount of generated H_2 till 16 hours, which is calculated for all cases with MPI. Except from very late start of injection more than 90 minutes after CET > 400 °C, all investigated cases show lower amount of hydrogen than for SBLOCA without any AMM. In general, injection to the hot leg shows higher total H_2 generation than cold leg injection. This can be explained in such a way, that for hot leg MPI, the coolant is directly injected to the hottest part of the core. The evaporation of the coolant provides a strong source of steam for cladding oxidation. Furthermore, the cool-down of the core is slower due to the slower reflooding process, most significant for hot leg injection without MPI (independent on the conditions at the start of the MPI). The preferred strategy from the release of fission products point of view, delayed PSD with immediate start of the hot leg MPI, also shows the lowest releases of hydrogen till 37 minutes after CET > 400 °C. Later on, between 40 and 70 minutes after CET > 400°C, the H_2 releases found for this strategy are up to 45 % higher than the releases found for cold leg MPI.

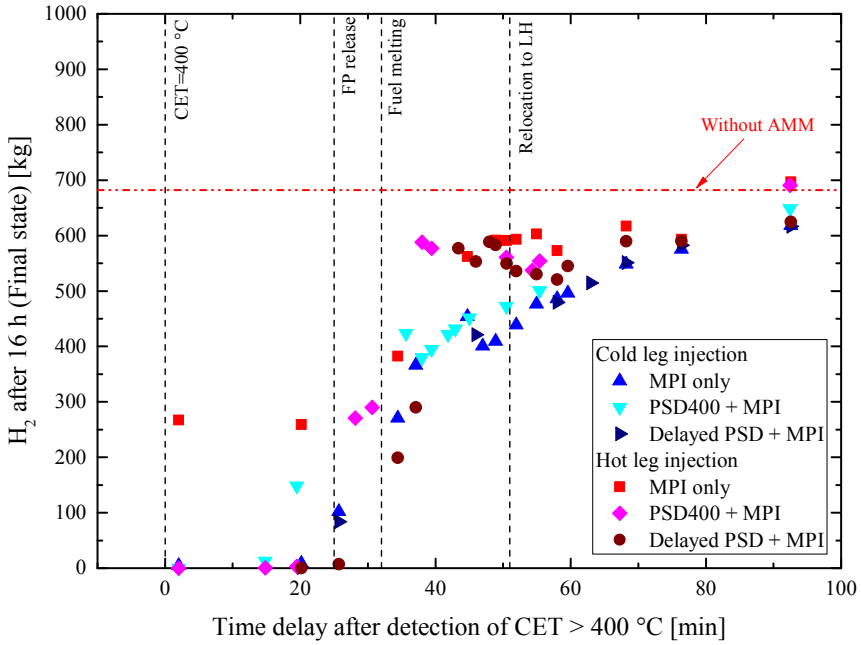

Fig. 19. H_2 generation depending on the start of the MPI (in terms of delay after detection of CET > 400 °C), point of injection and additional application of PSD.

Table 4 summarizes in a short overview, which events could be prevented in the course of the simulated SBLOCA transients by means of MPI without PSD or in combination with PSD. The core states in terms of reached CET or already molten core mass and the corresponding times are given. The simulations reveal that PSD is needed for prevention of fission product release (PSD + early enough MPI).

From all investigated options, mobile pump injection to hot leg in combination with delayed PSD, applied at the same time when the pump is available, is the optimal variant. According to the code results, by following this strategy, the operator will have the longest time to prevent the occurrence of FP release (until MPI started at 3 h 21 min), to prevent the occurrence of fuel melting (until MPI started at 3 h 27 min), or to prevent relocation of the core to lower head (until MPI started at 3 h 50 min). Following this strategy will lead to a bit reduced time margin to prevent vessel failure (only possible till MPI activated at 4 h 1 min, instead till 4 h 17 min as in case of hot leg injection without PSD). However, for very late times (mobile pump available beyond 4 hours), the strategy could be to start the MPI without application of PSD.

Table 4. Predicted latest possible start of the MPI to prevent the occurrence of selected events in the course of the investigated severe accident transient. (Times given as h:min).

Simulation set		#1	#3	#2	#4	#5	#6
MPI into		Cold leg	Hot leg	Cold leg	Hot leg	Cold leg	Hot leg
PSD		No	No	Yes	Yes	Yes	Yes
PSD initiated		-	-	CET > 400 °C	CET > 400 °C	Together with MPI	Together with MPI
Predicted latest possible start of MPI to :	… prevent fission product release	Not possible to prevent	Not possible to prevent	CET = 400 °C	CET = 400 °C	CET = 400 °C	CET = 650 °C
				3:03	3:03	3:03	3:21
	… prevent melting of fuel	CET = 650°C	Not possible to prevent	CET = 400°C	CET = 650 °C	CET = 650 °C	0.6 % core melt (CET ≈ 830 °C)
		3:21		3:03	3:16	3:21	3:27
	… prevent relocation to lower head	11 % core melt	3 % core melt	0.6 % core melt	13 % core melt	12 % core melt	18 % core melt
		3:46	3:35	3:21	3:40	3:47	3:50
	… prevent RPV failure (plastic rupture model)	48 % core melt	55 % core melt	30 % core melt	42 % core melt	12 % core melt*	42 % core melt
		4:10	4:17	3:46	3:56	3:47	4:01

* No statement could be made in the range between 12 % and 30 % (due to code termination).

6. Conclusions

The analyses of the code results for the investigated SBLOCA scenario showed, that if the sump injection fails in the Konvoi-like PWR after depletion of the flooding pools, the primary circuit is heated-up and the core starts to melt at approx. 3 h 20 min.

To prevent the occurrence of core melting or to mitigate its consequences, injection to the primary circuit by a mobile fire pump system with a maximum pump head of 16.5 bar has been investigated by in total 6 sets of ATHLET-CD calculations with varied injection point (cold leg vs. hot leg injection) and without or with additional primary side depressurization. Furthermore, two types of PSD initiation procedures were assessed: PSD performed at 400 °C CET according to standard procedures, despite the fact, that the mobile pump may not be available to inject, or, as second option, a delayed PSD until the moment, when the applied mobile pump is available to inject immediately. In total, 110 simulations were performed with ATHLET-CD Mod 3.0 Cycle A, from which 30 had to be excluded due to code terminations.

The simulations showed that MPI significantly reduces the amount of released fission products and hydrogen, if it is started within 75 minutes after reaching a CET > 400 °C. The code simulations also revealed that MPI as single measure is not sufficient to prevent the release of fission products in the case of the investigated SBLOCA transient. The main reason here is the primary pressure increase above the maximum pump head of the mobile pump after stop of ECCS injection and therefore less-efficient or temporary interrupted injection.

In case of MPI without PSD, no fuel melting was predicted if cold leg MPI is started at latest when CET reaches 650 °C (approximately 20 minutes after CET > 400 °C), and relocation to lower head can be prevented till 45 minutes after CET > 400 °C. Without PSD, injection to hot leg was less efficient, showed the longest duration for vessel reflooding and could not prevent fuel melting. Therefore, hot leg MPI without PSD is not recommended.

The application of additional PSD enhanced the efficiency of the mobile pump and significantly accelerated the reflooding process (in case of early activation, time needed for reflooding could be reduced from more than 3 hours till approx. 40 minutes). An injection strategy with a delayed PSD (delayed till the mobile pump is available to inject) and MPI to hot leg, immediately started after PSD, provides the most effective cooling of the core until approximately 50 minutes after CET exceeded 400 °C, with lowest fission product releases and longest grace time to prevent melt relocation to lower head. This strategy also shows lowest hydrogen releases till approx. 35 minutes after CET exceeded 400 °C. Later on, up to 45 % higher hydrogen is released compared to cold leg injection.

Late injection by mobile pump to the RCS in cases with corium relocated to lower head can help to stabilize and cool-down the lower head molten pool. The implemented in ATHLET-CD plastic rupture model was used to assess failure of the vessel in all investigated SBLOCA scenarios (low pressure). This model predicts no failure of the vessel, if injection is started within 1 hour after CET > 400 °C (for cases without PSD or delayed PSD with hot leg injection).

Further improvements of the model are envisaged. The user defined criterion for melt relocation should be substituted by a more detailed modelling approach for core molten pool crust failure and a model for failure of the lower core plate. The model should be extended by a containment model to take into account the pressure increase of containment (see discussion in (Wilhelm et al., xxxx)). The leak orientation, location and size need to be varied to investigate their influence to the transient and mobile pump injection. To simulate cases with pump injection to an intact loop, the triple loop has to be split into individual loops.

Kozmenkov et al. (2017) have shown that severe accident scenarios can be analysed using statistical methods developed for design-basis-accidents. It would be of interest to apply such an approach to the scenario investigated in our paper.

Furthermore, the performed ATHLET-CD code simulations contribute to the code assessment for scenarios with core degradation. The detected code errors are transferred to the code developers and are currently under discussion. In order to be able to investigate scenarios with injection to partly molten core and resulting large temperature gradients, the code stability need to be improved.

Abbreviations

AMM	Accident management measure
ATHLET(-CD)	Analyse der Thermohydraulik von Lecks und Transienten / Analysis of thermal-hydraulics of leak and transients (with core degradation)
CET	Core exit temperature
CL	Cold leg
DG	Diesel generator
ECC	Emergency core cooling
ECCS	Emergency core cooling system
FP	Fission products
GRS	Gesellschaft für Anlagen- und Reaktorsicherheit (GRS) gGmbH
HA	Hydro-accumulator
HL	Hot leg
HPIS	High pressure injection system
LH	Lower head
LPIS	Low pressure injection system
LOCA	Loss-of-coolant accident
MCP	Main coolant pump
MPI	Mobile pump injection
PSD	Primary side depressurization
PWR	Pressurized water reactor
RCS	Reactor cooling system
RPV	Reactor pressure vessel
SAMG	Severe accident management guidelines
SBLOCA	Small-break loss-of-coolant accident
SBO	Station blackout
WASA-BOSS	Weiterentwicklung und Anwendung von Severe Accident Codes – Bewertung und Optimierung von Störfallmaßnahmen (Further Development and Application of Severe Accident Codes – Assessment and Optimization of Accident Management Measures)

Acknowledgements

This work was performed within the WASA-BOSS project funded by the German Federal Ministry of Education and Research under project number 02NUK028B. The authors of this publication are responsible for its content.

The authors would like to express their gratitude to the ATHLET(-CD) developers' team at GRS.

References

Albert Ziegler GmbH, 2014. PFPN 10-1000/10-1500 ULTRA Power 4 [WWW Document]. https://www.ziegler.de/de/produkte/Loeschsysteme/tragkraftspritzen/pfpn-10-1000-10-1500-ultra-power-4, accessed 22.12.2017.

Altstadt, E., 2012. Lower head failure, in: Sehgal, B.R. (Ed.), Nuclear safety in light water reactors, 1st ed. Elsevier/Academic Press, Amsterdam, Boston.

Austregesilo, H., Bals, C., Hora, A., Lerchl, G., Romstedt, P., Schöffel, P., von der Cron, D., Weyermann, F., 2012. ATHLET Mod 3.0 Cycle A – Models and Methods, GRS-P-1 / Vol. 3 Rev. 3. Gesellschaft für Anlagen- und Reaktorsicherheit (GRS) gGmbH.

Austregesilo, H., Bals, C., Hollands, T., Köllein, C., Luther, W., Schubert, J.-D., Trambauer, K., Weber, S., 2013. ATHLET-CD Mod 3.0 Cycle A – User's Manual, GRS-P-4 / Vol. 1. Gesellschaft für Anlagen- und Reaktorsicherheit (GRS) gGmbH.

Autrusson, B., Combescure, A., 1999. Lower head thermo-mechanical behaviour, Workshop for In-Vessel Core Debris Retention and Coolability, 3-6 March 1998, Garching.

Bals, C., Köllein, C., Cester, F., Hollands, T., Luther, W., Schubert, J.D., Weber, S., 2012. Entwicklung von Kühlkreislaufmodellen zur Spätphase von Kernschmelzeunfällen (ATHLET-CD und ASTEC) Abschlussbericht; Reaktorsicherheitsforschung-Vorhabens Nr. RS1187, GRS-A-3646. Gesellschaft für Anlagen- und Reaktorsicherheit (GRS) gGmbH, Köln.

DIN 14811-1, 1990. DIN 14811-1, Fire hoses; requirements, testing, treatment. Beuth Verlag, Berlin.

Gomez-Garcia-Torano, I., Espinoza, V.H.S., Stieglitz, R., 2017a. Investigation of SAM measures during selected MBLOCA sequences along with Station Blackout in a generic Konvoi PWR using ASTECV2.0. Annals of Nuclear Energy 105, pp. 226–239.

Gomez-Garcia-Torano, I., Sanchez-Espinoza, V.H., Stieglitz, R., Queral, C., 2017b. Analysis of primary bleed and feed strategies for selected SBLOCA sequences in a German Konvoi PWR using ASTEC V2.0. Annals of Nuclear Energy 110, pp. 818–832.

Jobst, M., Wilhelm, P., Kozmenkov, Y., Kliem, S., Trometer, A., Buck, M., Kretzschmar, F., Dietrich, P., 2016. WASA-BOSS Weiterentwicklung und Anwendung von Severe Accident Codes – Bewertung und Optimierung von Störfallmaßnahmen: Meilensteinbericht M35 – Simulation postulierter schwerer Störfälle in deutschen DWR. Helmholtz-Zentrum Dresden-Rossendorf, Institut für Ressourcenökologie.

Jobst, M., Kliem, S., Kozmenkov, Y., Wilhelm, P., 2017a. Verbundprojekt WASA-BOSS: Weiterentwicklung und Anwendung von Severe Accident Codes – Bewertung und Optimierung von Störfallmaßnahmen; Teilprojekt B: Druckwasserreaktor-Störfallanalysen unter Verwendung des Severe-Accident-Code ATHLET-CD, HZDR-080, Wissenschaftlich-Technische Berichte. Helmholtz-Zentrum Dresden-Rossendorf, Institut für Ressourcenökologie.

Jobst, M., Wilhelm, P., Kliem, S., 2017b. Application of ATHLET-CD code for simulation of SBLOCA 50 cm² severe accident scenario for a generic German PWR, 8th European Review Meeting on Severe Accident Research, Warsaw.

Kliem, S., Hoffmann, A., Jobst, M., Kozmenkov, Y., Wilhelm, P., 2017. Activity report on the use of GRS codes in the year 2016. Helmholtz-Zentrum Dresden-Rossendorf, Institut für Ressourcenökologie.

Kozmenkov, Y., Jobst, M., Kliem, S., Schäfer, F., Wilhelm, P., 2017. Statistical Analysis of the Early Phase of SBO Accident for PWR. Nuclear Engineering and Design 314, pp. 131–141.

Lerchl, G., Austregesilo, H., Glaeser, H., Hrubisko, M., Luther, W., 2012a. ATHLET Mod 3.0 Cycle A – Validation, GRS-P-1 / Vol. 3 Rev. 3. Gesellschaft für Anlagen- und Reaktorsicherheit (GRS) gGmbH.

Lerchl, G., Austregesilo, H., Schöffel, P., von der Cron, D., Weyermann, F., 2012b. ATHLET Mod 3.0 Cycle A – User's manual, GRS-P-1 / Vol. 1 Rev. 6. Gesellschaft für Anlagen- und Reaktorsicherheit (GRS) gGmbH.

Loeffler, M., Braun, M., Plank, H., 2012. SARNET2 Two-days Course on Severe Accidents Phenomenology and Management. KIT, 11th of July 2012, Part 9. SAMGs I: General Overview. AREVA NP GmbH.

Pandazis, P., 2017. Electronic mail correspondence regarding the vessel failure models and the corresponding equations implemented in ATHLET-CD.

Reinke, N., Erdmann, W., Nowack, H., Sonnenkalb, M., 2010. Vergleichende Unfallanalysen für einen DWR vom Typ KONVOI mit den Integralcodes ASTEC V1.33 und MELCOR 1.8.6 Vorhaben RS 1180 (AP 5.1), GRS-A-3559. Gesellschaft für Anlagen- und Reaktorsicherheit (GRS) gGmbH, Köln.

RSK, 2005. RSK-Empfehlung, Anforderungen an die Nachweisführung bei Kühlmittelverluststörfall-Analysen, 385. RSK-Sitzung (20./21. 07. 2005).

Schaaf, K., Sievers, J., Müller, C., 1999. Entwicklung und Verifikation von Modellen zur Beschreibung der Wechselwirkung Debris-Reaktordruckbehalterwand, GRS-A-2749. Gesellschaft für Anlagen- und Reaktorsicherheit (GRS) gGmbH.

Schäfer, F., Tusheva, P., Kozmenkov, Y., Kliem, S., 2014. WASA-BOSS Weiterentwicklung und Anwendung von Severe Accident Codes – Bewertung und Optimierung von Störfallmaßnahmen: LOCA50 – Sensitivity simulations with ATHLET Mod 3.0 Cycle A. Helmholtz-Zentrum Dresden Rossendorf, Institut für Ressourcenökologie.

Trambauer, K., Austregesilo, H., Bals, C., Cester, F., Deitenbeck, H., Hora, A., Lerchl, G., Schubert, J.D., Voggenberger, T., 2004. Weiterentwicklung des Rechenprogrammsystems ATHLET/ATHLET-CD, GRS-A-3215. Gesellschaft für Anlagen- und Reaktorsicherheit (GRS) gGmbH.

Trometer, A., Buck, M., Starflinger, J., 2014. Investigations on Cooling Possibilities of a Degraded Core in a MBLOCA Scenario for a German PWR with ATHLET-CD, The 19th Pacific Basin Nuclear Conference (PBNC 2014), August 24-28, 2014, Vancouver, British Columbia, Canada.

Trometer, A., Strätz, M., Buck, M., Starflinger, J., 2015. Parametric study on a KONVOI MB-LOCA scenario for the determination of coolability parameters., 46th Annual Meeting on Nuclear Technology (AMNT), May 5 - 7, 2015, Berlin, Germany.

Trometer, A., 2016. Investigations on the flooding behaviour of a partially degraded reactor core. PhD Thesis, Fakultät Energie-, Verfahrens- und Biotechnik. University of Stuttgart.

Tusheva, P., Schäfer, F., Kozmenkov, Y., Kliem, S., Hollands, T., Trometer, A., Pohlner, G., Buck, M., 2014. WASA-BOSS Weiterentwicklung und Anwendung von Severe Accident Codes – Bewertung und Optimierung von Störfallmaßnahmen: Milestone Report M32: Simulation of postulated accidents / severe accidents in German NPPs. Helmholtz-Zentrum Dresden-Rossendorf, Institut für Ressourcenökologie.

Tusheva, P., Schäfer, F., Kozmenkov, Y., Kliem, S., Hollands, T., Trometer, A., Buck, M., 2015. WASA-BOSS: ATHLET-CD Model for Severe Accident Analysis for a Generic KONVOI Reactor. Atw. Internationale Zeitschrift fuer Kernenergie 60, pp. 442–447.

Vayssier, G., 2012. Severe accident management guidlines (SAMG), in: Sehgal, B.R. (Ed.), Nuclear safety in light water reactors, 1st ed. Elsevier/Academic Press, Amsterdam Boston.

Wilhelm, P., Jobst, M., Kozmenkov, Y., Kliem, S., xxxx. Severe Accident Management Measures for a Generic German PWR. Part I: Station Blackout (submitted together with Part II paper). Annals of Nuclear Energy.

Wolfert, K., 1979. Die Berücksichtigung thermodynamischer Nichtgleichgewichtszustände bei der Simulation von Druckabsenkungsvorgängen. PhD Thesis. TU Munich.